

Resonant cyclotron scattering in pulsar magnetospheres and its application to isolated neutron stars

Hao Tong¹, Ren Xin Xu², Qiu He Peng¹ and Li Ming Song³

¹ Department of Astronomy, Nanjing University, Nanjing 210093, China; haotong@nju.edu.cn

² Department of Astronomy, Peking University, Beijing 100871, China

³ Institute of High Energy Physics, Chinese Academy of Sciences, Beijing 100049, China

Received [year] [month] [day]; accepted [year] [month] [day]

Abstract Resonant cyclotron scattering (RCS) in pulsar magnetospheres is considered. The photon diffusion equation (Kompaneets equation) for RCS is derived. The photon system is modeled three dimensionally. Numerical calculations show that there exist not only up scattering but also down scattering of RCS, depending on the parameter space. RCS's possible applications to the spectra energy distributions of magnetar candidates and radio quiet isolated neutron stars (INSs) are point out. The optical/UV excess of INSs may caused by the down scattering of RCS. The calculations for RX J1856.5-3754 and RX J0720.4-3125 are presented and compared with their observational data. In our model, the INSs are proposed to be normal neutron stars, although the quark star hypothesis is still possible. The low pulsation amplitude of INSs is a natural consequence in the RCS model.

Key words: radiation mechanism: nonthermal, scattering, stars: neutron, pulsars: general, pulsar: individual: RX J1856.5-3754, pulsar: individual: RX J0720.4-3125

1 INTRODUCTION

Three kinds of pulsar-like objects have additionally and greatly boosted up our knowledge about pulsar magnetospheres. They are anomalous X-ray pulsars and soft gamma-ray repeaters (magnetars candidates), radio quiet isolated neutron stars (INSs) (the magnificent seven), and rotating radio transients (RRATs). Figure 1 shows their positions on the $P - \dot{P}$ diagram. Our conventional picture of pulsar magnetospheres is provided by e.g. Goldreich & Julian (1969), Ruderman & Sutherland (1975), and Cheng et al. (1986) (for a recent review, see Kaspi et al. 2006), which is mainly about the open field line regions (OFLRs). Few people begin to realize that there could be interesting physics in the closed field line regions (CFLRs) of pulsar magnetospheres. For magnetars, it is proposed that there is strong and twisted magnetic field around the central star (Thompson et al. 2002; Lyutikov & Gavriil 2006). INSs are thought to be dead neutron stars, which provide a clear specimen for magnetospheric and cooling studies (Kaspi et al. 2006; Tong & Peng 2007; Tong et al. 2008). For RRATs, recent modeling also indicates interesting physics in CFLRs (Luo & Melrose 2007). The most direct evidence comes from the observations of the double pulsar system PSR J0737-3039A/B, and there could be also signatures of interesting physics in CFLRs of normal pulsars (Lyutikov 2008).

The interesting physics in pulsar CFLRs are mainly related to the plasmas there. Roughly speaking, the electron density in magnetar CFLRs is about 4-5 orders higher than the Goldreich-Julian density (Rea et al. 2008). In the case of RRATs, Luo & Melrose (2007) have proposed an idea of “pulsar

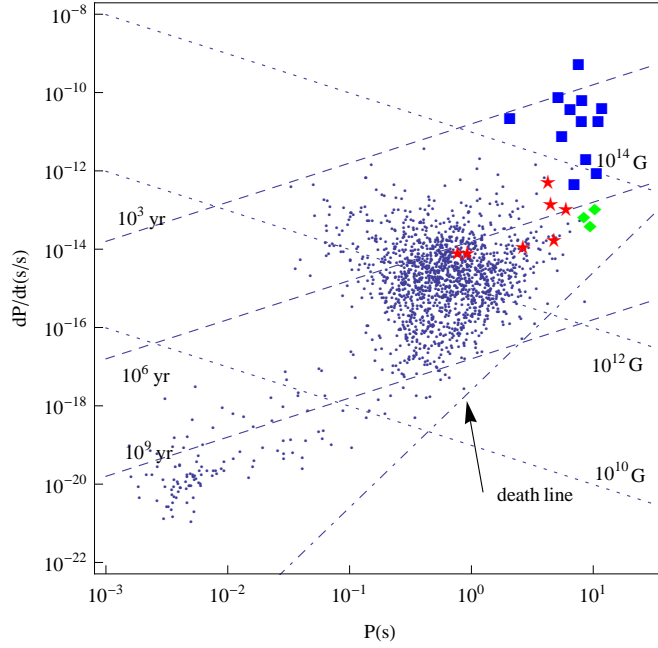


Fig. 1 $P - \dot{P}$ diagram of pulsars. Diamonds are for INSs (Haberl 2007; Kaplan & van Kerkwijk 2009). Stars are for RRATs (McLaughlin et al. 2006; McLaughlin et al. 2009). Magnetar (squares) and radio pulsar (dots) data are from ATNF (<http://www.atnf.csiro.au/research/pulsar/psrcat/>). The dotdashed line is the constant potential line $V = 1/3 \times 10^{12}$ V.

radiation belt”, like the radiation belt of the earth. Noting the similarities between INSs and magnetars/RRATs, we suggest that there could also be plasmas in INS CFLRs with number density greatly higher than the Goldreich-Julian density (i.e. the electron blanket, see Wang et al. 1998; Ruderman 2003). We observed three similarities between INSs and magnetars/RRATs:

1. Most of them are long period pulsars with spin periods about 10 seconds;
2. They all show a non-atomic Planckian spectrum;
3. They all have large or relatively large spin-down rates (indicating possible higher fields).

With these similarities, we suggest that the physics of these three kinds of objects should be similar, and that the very different observational manifestations could be resulted from a different parameter space and an evolution history.

In this paper we consider resonant cyclotron scattering (RCS) process in pulsar magnetospheres. In section two, a brief description of the RCS process and some basic formulas are given. Kompaneets equation for the RCS process is deduced in section three. Numerical calculations are given in section four. The application to INSs is the topic of section five. In the last two sections, discussions and conclusions are summarized, respectively.

2 RESONANT CYCLOTRON SCATTERING

Near the neutron star surface, RCS of photons is more important than Compton scattering (Ruderman 2003). It has the following three points.

1. Given the magnetic field, the scattering occurs only at a specific frequency and vice versa. Given the frequency, the scattering occurs only at a specific location in the pulsar magnetosphere. At the

resonant frequency, the cross section is about 8 orders larger than the Thomson cross section for typical magnetic field 10^{12} G.

2. The momentum is conserved only along the z-direction (direction of the magnetic field). The field may absorb or contribute perpendicular momentum.
3. The particle distribution is strongly affected by the field. The perpendicular motion is suppressed while particles can move freely along field lines. Therefore the electron distribution is 1D.

The soft X-ray spectrum of magnetars may be the result of RCS of surface thermal emission (Rea et al. 2008). One has three ways dealing with scattering problems (including resonant scattering). One is solving the radiation transfer equation directly (e.g. Lyutikov & Gavriil 2006), the second is doing Monte Carlo simulations (Fernandez & Thompson 2007; Nobili et al. 2008), and the third is introducing photon diffusion equation (Kompaneets equation) as in the Compton scattering case (e.g. Rybicki & Lightman 1979). However, the Kompaneets equation for RCS has not been developed yet. Considering its importance in magnetar soft X-ray emission, we present a Kompaneets equation method for the RCS process in this paper. Also improved approximations are employed. We find that it may account for the optical/UV excess of INSs.

Previous solution provided by Lyutikov & Gavriil (2006) has three problems which should be improved. The three problems are:

1. It's a one dimensional treatment. Photons can only propagate forward or backward. All the calculations and arguments there are valid only in the 1D case. This will cause two additional problems.
2. The angular dependence of the RCS cross section is smeared out. The rigorous expression is eq. (3) which we will discuss in the following.
3. The down scattering of photons is dropped. In the 1D case, the phase space volume is proportional to $\propto p$. While in the 3D case it is proportional to $\propto p^3$. Noting that photons are bosons, the key difference between the 3D and 1D case is that there is no Bose-Einstein condensation in the later case (Pathria 2003). While the down scattering is Bose-Einstein condensation of photons in the low energy state (Liu et al. 2004; Sunyaev & Titarchuk 1980), therefore it can not be handled in the 1D case. Then it is not surprising that the authors found a net up scattering of transmitted flux. It is the approximations they employed that matters. We try to provide a 3D treatment of the photon system in this paper.

Before going to deduction details, some basic formulas should be given at first (You et al. 1997). Cyclotron frequency of electrons in a given magnetic field is

$$\nu_B = \frac{1}{2\pi} \frac{eB(r)}{m_e c}, \quad (1)$$

$$\omega_B = \frac{eB(r)}{m_e c}, \quad (2)$$

where ν_B is the local cyclotron frequency, ω_B is the angular frequency $\omega_B = 2\pi\nu_B$, e is the electron charge (absolute value), $B(r)$ is the local magnetic field, r is the distance from the point to the center of the star, m_e is the electron rest mass, and c is the speed of light. When $\nu = \nu_B$, where ν is the photon frequency, RCS occurs. The differential cross section is

$$d\sigma_{\text{RCS}} = \frac{3r_e c}{32} (1 + \cos^2 \theta)(1 + \cos^2 \theta') \phi(\nu - \nu_B) d\Omega', \quad (3)$$

where r_e is the classical electron radius, θ is the angle between the incoming photon and the local magnetic field, θ' denotes the angle of the outgoing photon, $d\Omega'$ is the solid angle of the outgoing photon, and $\phi(\nu - \nu_B)$ is the Lorentz line profile function, which acts like a Dirac delta function

$$\phi(\nu - \nu_B) = \frac{\Gamma/4\pi^2}{(\nu - \nu_B)^2 + (\Gamma/4\pi)^2}. \quad (4)$$

Note that Γ is the natural width

$$\Gamma = \frac{4e^2\omega_B^2}{3m_e c^3}. \quad (5)$$

The Lorentz line profile function has the normalization condition

$$\int_{-\infty}^{+\infty} \phi(\nu - \nu_B) d\nu = 1. \quad (6)$$

Performing the angular integral gives the total cross section

$$\sigma_{\text{RCS}} = \frac{1}{2}\pi r_e c (1 + \cos^2 \theta) \phi(\nu - \nu_B), \quad (7)$$

which depends on frequency.

In the case of pulsars, dipole magnetic field is always a good approximation. The magnetic field at radius r is

$$B(r) = B_p \left(\frac{R}{r} \right)^3, \quad (8)$$

where B_p is the magnetic field at the surface of the neutron star, and R is the neutron star radius. Given the photon frequency ν , the radius at which RCS occurs is

$$r_{\text{RCS}} = \left(\frac{\nu_{B_p}}{\nu} \right)^{1/3} R, \quad (9)$$

where ν_{B_p} is the cyclotron frequency at the star surface $\nu_{B_p} = \frac{1}{2\pi} \frac{eB_p}{m_e c}$ (only photons with frequency smaller than ν_{B_p} will encounter RCS). For photons in the soft X-ray band $1 \text{ keV} < h\nu < 10 \text{ keV}$ (with h is Planck's constant), we are only considering a specific frequency range $\nu_1 < \nu < \nu_2$. The scattering occurs in a finite space range $r_2 < r < r_1$, where r_2 is the scattering radius corresponding to frequency ν_2 , and r_1 corresponding to frequency ν_1 . We assume that there are bulk of electrons filling the space between r_2 and r_1 . Beyond r_1 there may also be bulk of electrons, but it is less related to the observations in the frequency range ν_1 to ν_2 . Finally we introduce the optical depth of RCS

$$\tau_{\text{RCS}} = \int N_e \sigma_{\text{RCS}} dr = \tau_0 (1 + \cos^2 \theta), \quad (10)$$

where N_e is the electron number density (assuming homogenous),

$$\tau_0 = \frac{\pi e^2 N_e r_{\text{RCS}}}{6m_e c \nu}. \quad (11)$$

The optical depth also depends on frequency $\propto 1/\nu^{4/3}$. In the following sections, all optical depth are referred to their value at the lower frequency boundary, i.e. optical depth at ν_1 . During the integration of eq. (10), the spatial dependence of magnetic field (eq. (8)) is taken into consideration. This will be used in the numerical calculation section.

3 KOMPANEETS EQUATION FOR RESONANT CYCLOTRON SCATTERING

We formulate our deduction analogous to that of Kompaneets equation for Compton scattering (e.g. Rybicki & Lightman 1979; You 1998; Padmanabhan 2000).

Denote the initial and final state of the scattering as (p_z, ν, \mathbf{n}) and $(p'_z, \nu', \mathbf{n}')$, respectively, with p_z is the initial electron momentum in the z -direction, ν the initial photon frequency, \mathbf{n} the propagation direction of the incoming photon, and a prime denotes the corresponding quantity of the outgoing particles. In strong magnetic field, electron motions perpendicular to the magnetic field are celled into Landau energy levels. Almost all the electrons are in the ground state (You et al. 1997). And we only

consider photons in the ground state before and after the scattering (Herold 1979). According to energy-momentum conservation in the non-relativistic case, we have

$$h\nu + \frac{p_z^2}{2m_e} = h\nu' + \frac{p_z'^2}{2m_e}, \quad (12)$$

$$\left(\frac{h\nu}{c} \cos \theta\right) + p_z = \left(\frac{h\nu'}{c} \cos \theta'\right) + p_z'. \quad (13)$$

It seems that we are dealing with a 1D distribution of electrons.

From the conservation of energy and momentum, we can calculate the frequency change after and before the scattering $\Delta = h(\nu' - \nu)/kT_e$, with k is Boltzmann's constant, and T_e the effect temperature of the electron system. Since we are dealing with non-relativistic electrons $kT_e \ll m_e c^2$, and consider typical photons in the X-ray band $h\nu \sim 1 \text{ keV} \ll m_e c^2$, the frequency change is very small $\Delta \ll 1$. Therefore only considering first order terms of Δ , we have

$$\Delta = -\frac{x p_z}{m_e c} (\cos \theta - \cos \theta'), \quad (14)$$

where x is the dimensionless frequency $x = h\nu/kT_e$. The above expression is accurate to an order of $O(\frac{h\nu}{m_e c^2} \frac{h\nu}{kT_e})$, which is negligible in the case of magnetars and INSs. The validity of Kompaneets equation method in the nonrelativistic case is well established (e.g. eq.(7.53) in Rybicki & Lightman 1979).

Let $n(\nu)$ denotes the occupation number per photon state of frequency ν . We denote the transition probability from an initial state (p_z, ν, \mathbf{n}) to a final state $(p_z', \nu', \mathbf{n}')$ as dW . Note that the transition probability is a microscopic quantity, we always have $dW' = dW$. Since electrons move freely along the z-direction, we describe the electron system as a 1D Maxwellian distribution. The number of electrons with momentum in the range $p_z - p_z + dp_z$ is $f(p_z)dp_z$, with

$$f(p_z) = N_e (2\pi m_e kT_e)^{-1/2} e^{-p_z^2/2m_e kT_e}. \quad (15)$$

The evolution of the photon spectrum is described by the Boltzmann equation (Rybicki & Lightman 1979)

$$\left(\frac{\partial n}{\partial t}\right)_{\text{RCS}} = \int dp_z \int dW [f(p_z') n' (1+n) - f(p_z) n (1+n')]. \quad (16)$$

where a subscript RCS means the change of occupation number is caused by RCS, n and n' are abbreviated forms of $n(\nu)$ and $n(\nu')$, respectively. For non-relativistic electrons, the frequency change is small $\Delta \ll 1$, we can expand eq. (16) to terms of Δ^2 and neglect higher order terms. The change of photon occupation number becomes

$$\begin{aligned} \left(\frac{\partial n}{\partial t}\right)_{\text{RCS}} &= \left[\frac{\partial n}{\partial x} + n(1+n)\right] \int dp_z \int dW f(p_z) \Delta \\ &+ \left[\frac{1}{2} \frac{\partial^2 n}{\partial x^2} + \frac{\partial n}{\partial x} (1+n) + \frac{1}{2} n(1+n)\right] \int dp_z \int dW f(p_z) \Delta^2. \end{aligned} \quad (17)$$

We denote the two integrals by

$$I_1 = \int dp_z \int dW f(p_z) \Delta \quad (18)$$

$$I_2 = \int dp_z \int dW f(p_z) \Delta^2, \quad (19)$$

and then eq. (17) becomes

$$\begin{aligned} \left(\frac{\partial n}{\partial t}\right)_{\text{RCS}} &= \left[\frac{\partial n}{\partial x} + n(1+n)\right] I_1 \\ &+ \left[\frac{1}{2}\frac{\partial^2 n}{\partial x^2} + \frac{\partial n}{\partial x}(1+n) + \frac{1}{2}n(1+n)\right] I_2. \end{aligned} \quad (20)$$

Using the conservation of photon numbers can greatly simplify the subsequent calculations.

The number of photons is conserved during the scattering process. Thus we have the continuity equation of $n(x)$ in the frequency space

$$\frac{\partial n}{\partial t} = -\nabla \cdot \mathbf{j}, \quad (21)$$

where \mathbf{j} is the photon flux in the frequency space. Assuming $n(x)$ is isotropic (the validity of the isotropic assumption will be discussed in the appendix), we have

$$\frac{\partial n}{\partial t} = -\frac{1}{x^2}\frac{\partial}{\partial x}(x^2 j) \quad (22)$$

A comparison between eq. (22) and eq. (20) gives that the flux j must have the form (Rybicki & Lightman 1979)

$$j(x) = g(x) \left[\frac{\partial n}{\partial x} + n(1+n)\right]. \quad (23)$$

Note that in equilibrium conditions, $n(x) = (e^x - 1)^{-1}$, $\frac{\partial n}{\partial x} = -n(1+n)$, we have no ‘‘photon flux’’ in the frequency space, $j = 0$. This is a necessary condition. The same condition can be used to check the validity of other forms of diffusion equation (e.g. Liu et al. 2004). Substituting the above equation into eq. (22) we have

$$\frac{\partial n}{\partial t} = -\frac{1}{x^2}\frac{\partial}{\partial x} \left\{ x^2 g(x) \left[\frac{\partial n}{\partial x} + n(1+n)\right] \right\} \quad (24)$$

A comparison between the coefficient of $\frac{\partial^2 n}{\partial x^2}$ in eq. (24) and eq. (20) gives $g(x)$

$$g(x) = -\frac{1}{2}I_2. \quad (25)$$

Finally the Kompaneets equation for RCS has the form

$$\frac{\partial n}{\partial t} = \frac{1}{x^2}\frac{\partial}{\partial x} \left\{ x^2 \frac{1}{2}I_2 \left[\frac{\partial n}{\partial x} + n(1+n)\right] \right\}. \quad (26)$$

We only need to calculate the integral I_2 .

Substituting the equation of frequency change eq. (14) into the definition of the integral I_2 eq. (19), first performing the integral of momentum p_z , we obtain

$$I_2 = \int dW x^2 N_e \frac{kT_e}{m_e c^2} (\cos \theta - \cos \theta')^2 \quad (27)$$

The transition probability is directly related to the cross section

$$\begin{aligned} dW &= cd\sigma_{\text{RCS}} \\ &= c\frac{3r_e c}{32}(1 + \cos^2 \theta)(1 + \cos^2 \theta')\phi(\nu - \nu_B)d\Omega'. \end{aligned} \quad (28)$$

Since we are dealing with non-relativistic electrons, the cross section can be approximated by its value in the electron rest frame. Performing the integral over $d\Omega'$, we have

$$I_2 = 2x^2 N_e \sigma_{\text{RCS}} c \frac{kT_e}{m_e c^2} g_\theta, \quad (29)$$

where g_θ is an angle dependent factor $g_\theta = \frac{1}{5} + \frac{1}{2} \cos^2 \theta$. Finally the Kompaneets equation for RCS is

$$\left(\frac{\partial n}{\partial t} \right)_{\text{RCS}} = \frac{kT_e}{m_e c^2} \frac{1}{x^2} \frac{\partial}{\partial x} \left\{ x^4 N_e \sigma_{\text{RCS}} c g_\theta \left[\frac{\partial n}{\partial x} + n(1+n) \right] \right\}. \quad (30)$$

The cross section σ_{RCS} now depends on frequency, therefore it can not be taken out of the curly brackets. Except for this difference and an angle dependent factor g_θ , it is the same as the Kompaneets equation for Compton scattering.

4 NUMERICAL CALCULATIONS

Before we make numerical calculations of eq. (30), two integrations should be performed. Performing a space integral on both sides of eq. (30), employing the concept of optical depth as in eq. (10), we obtain the Kompaneets equation in the case of pulsars

$$\left(\frac{\partial n}{\partial t} \right)_{\text{RCS}} = \frac{kT_e}{m_e c^2} \frac{1}{x^2} \frac{\partial}{\partial x} \left\{ x^4 \frac{\tau_{\text{RCS}}}{r_1 - r_2} c g_\theta \left[\frac{\partial n}{\partial x} + n(1+n) \right] \right\}. \quad (31)$$

The expression $r_1 - r_2$ in the denominator is the range of integration. It is also the range of cyclotron scattering corresponding to the frequency range ν_1 to ν_2 . The space integration must be employed in order to eliminate the Dirac delta function in the RCS cross section.

There is an angular factor in the RCS optical depth τ_{RCS} , we denote it as $f_\theta = 1 + \cos^2 \theta$. To simplify the calculations, we use the average value of f_θ and g_θ

$$\overline{f_\theta} = \frac{4}{3} \quad (32)$$

$$\overline{g_\theta} = \frac{2}{5}. \quad (33)$$

Here $\overline{g_\theta} = \overline{f_\theta g_\theta} / \overline{f_\theta}$. From eq. (30) till now, we have performed two integrations. One is integration over space range, the other is averaging over the incoming angle. These two integrations are introduced in order to simplify the numerical calculations.

The Kompaneets equation for RCS is a pure initial value nonlinear partial differential equation. Solving the pure initial value problem follows the same routine as the mixed initial value and boundary value problem. In the case of Kompaneets equation for RCS, we have to be careful since we are working a semi-infinite domain, that is $0 < \nu < \infty$. In the real case, we are only interested in a finite frequency range (e.g. in the cases of magnetars, INSs). Therefore boundary conditions are needed.

The Kompaneets equation for RCS describes the diffusion of photons in the frequency space. It is related to the specific intensity as

$$I_\nu(t) = \frac{2h\nu^3}{c^2} n(\nu, t). \quad (34)$$

For a blackbody spectrum, the initial condition is¹

$$n(x, t = 0) = \frac{1}{\exp\left(\frac{x}{T_{\text{rad}}/T_e}\right) - 1}. \quad (35)$$

¹ We are considering a spherical shell of electrons, extending from r_2 to r_1 . When the radiation reaches the lower boundary r_2 , this is taken as $t = 0$. At r_2 , it is already several radii far away from the neutron star surface. The gravity there is already very weak. Therefore general relativistic effect is negligible when the radiation propagates from r_2 to r_1 .

Since we only consider pure scattering between electrons and photons, the number of photons is conserved. The choice of boundary conditions must guarantee this requirement. One guess is that there are no photons going in or out of the specified frequency range. Mathematically this is

$$\frac{\partial n(x, t)}{\partial x} + n(x, t)(1 + n(x, t)) = 0, \quad \text{when } x = x_1, x_2 \quad \text{for all } t. \quad (36)$$

Compare eq. (23) (Ross et al. 1978). During the numerical calculations, a simplified version is used²

$$\frac{\partial n(x, t)}{\partial x} = 0, \quad \text{when } x = x_1, x_2 \quad \text{for all } t. \quad (37)$$

In obtaining the final RCS modified spectrum, we use the random walk approximation. A photon entered the lower boundary r_2 escapes the outer boundary r_1 after an average diffusion time scale

$$t_{\text{dif}} = \tau_{\text{RCS}}(\nu_1)(r_1 - r_2)/c. \quad (38)$$

In the random walk approximation, $n(x, t_{\text{dif}})$ is the final output.

Figure 2 and figure 3 are the numerical results for up scattering and down scattering case, respectively. Figure 2 shows the result for typical parameters of magnetars. During the calculations, the magnetic field and stellar radius are chosen as typical values of $B = 4.4 \times 10^{14}$ G and $R = 10^6$ cm. It can reproduce a stiffened blackbody spectrum, therefore it may be applied to interpret magnetar soft X-ray spectrum. Figure 3 shows the calculation for typical parameters of INs with $B = 10^{13}$ G and $R = 10^6$ cm. It produces a spectrum with optical/UV excess. Therefore it may account for the optical/UV excess of INs.

The luminosity of photons³ (number of photons per unit time passing a fixed surface) is proportional to $\int_{x_1}^{x_2} x^2 n(x, t) dx$. We can calculate this integral before and after the scattering to check whether the number of photons is conserved during the calculations. In the down scattering case, the specified frequency range spans about three orders of magnitude. The number of photons changes less than five percent before and after the scattering. While in the up scattering case, the specified frequency range only spans one order of magnitude. If we insert boundary conditions at x_1 and x_2 , the number of photon is not conserved. It is because the specified frequency range is not wide enough. Therefore we insert boundary conditions “far away” from the specified frequency range, at $x_1/10$ and $15x_2$. The number of photons changes less than one thousandth.

5 APPLICATION TO ISOLATED NEUTRON STARS

ROSAT discovered seven radio quiet INs (Kaspi et al. 2006; Trümper 2005; for recent reviews see Haberl 2007; van Kerkwijk & Kaplan 2007). They all show featureless blackbody spectra, with low pulsation amplitude, and high X-ray to optical flux ratio. Their spectral energy distributions show that many of them have an optical/UV excess with a factor of several (Burwitz et al. 2001; Burwitz et al. 2003; Motch et al. 2003; Ho et al. 2007; van Kerkwijk & Kaplan 2007). Table 1 shows double blackbody fit of RX J1856.5-3754 (J1856 for short) and RX J0720.4-3125 (J0720 for short). In interpreting their optical/UV excess, the emission radius is either too small or too big for reasonable star radius. Several theoretical models have been proposed (Motch et al. 2003; Ho et al. 2007; Trümper 2005). Considering the discrepancy between current theory and observations, we try to provide an alternative one, in which the optical/UV excess of INs may due to magnetospheric processes, i.e. due to down scattering of RCS when the surface emission passing through the pulsar magnetosphere.

² Take the equilibrium condition for example. $n(\nu) = \frac{1}{e^{h\nu/kT_{\text{rad}}} - 1}$. At the upper frequency boundary $h\nu_2 \gg kT_{\text{rad}}$, $n \ll 1$, the third type boundary condition is reduced to the second type. At the lower boundary $h\nu_1 \leq kT_{\text{rad}}$, this is a poor approximation. However, the number of low energy photons is proportional to $x^2 n(x) dx \propto x^2 \ll 1$, which is also of a small amount. Therefore we employ the simplified version of boundary conditions. The validity of this simplified approximation is discussed at the end of this section.

³ luminosity=flux \times area= $\pi \frac{L\nu}{h\nu} \left(\frac{R}{r}\right)^2 4\pi r^2$, then integrate over the specified frequency range.

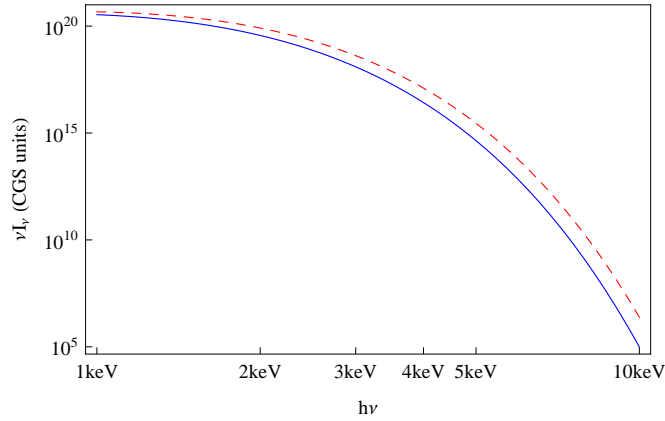


Fig. 2 Modified blackbody spectrum due to resonant cyclotron scattering, up scattering case, for typical parameters of magnetars. The initial blackbody temperature is 0.2 keV, the electron temperature is 10 keV. The solid line is the initial blackbody spectrum. The dashed line is the RCS modified spectrum with optical depth $\tau_{\text{RCS}}(\nu_1) = 2$. The specified frequency range is $(\nu_1, \nu_2) = (1 \text{ keV}, 10 \text{ keV})$. The model parameters are $(x_1, x_2) = (0.1, 1)$, $(r_2, r_1) = (8.0, 17) \times 10^6 \text{ cm}$.

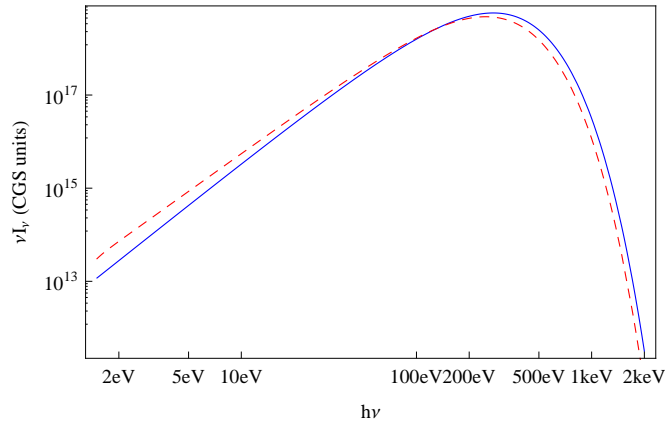


Fig. 3 Modified blackbody spectrum due to resonant cyclotron scattering, down scattering case, for typical parameters of isolated neutron stars. The initial blackbody temperature is 70 eV, the electron temperature is 26 eV. The solid line is the initial blackbody spectrum. The dashed line is the RCS modified spectrum with optical depth $\tau_{\text{RCS}}(\nu_1) = 1000$. The specified frequency range is $(\nu_1, \nu_2) = (1.5 \text{ eV}, 2 \text{ keV})$. The model parameters are $(x_1, x_2) = (0.058, 77)$, $(r_2, r_1) = (3.9, 42) \times 10^6 \text{ cm}$.

Figure 4 and figure 5 show the RCS modified blackbody spectrum in the case of J1856 and J0720, respectively. It can account for the optical/UV excess in J1856 and J0720 quite well. We assume that the initial spectrum is blackbody. When passing through the pulsar magnetosphere, it is modified by the RCS process. Therefore the final observed spectrum is a modified blackbody, with optical/UV excess due to down scattering of RCS. Four parameters are needed: the initial body temperature, the temperature of

Table 1 Double Blackbody Fit to INS Spectral Energy Distributions. T_X is the high temperature component (X-ray), T_O is the low temperature component (optical/UV), seen at infinity. R_X and R_O are the corresponding emission radius, seen at infinity. Here all numbers are only estimated values, no error bars are given, which are taken from van Kerkwijk & Kaplan (2007).

	kT_X eV	R_X km	kT_O eV	R_O km	distance pc
J1856	63	5.9	26	24.3	161
J0720	85.7	5.7	35.4	23.5	330

Table 2 RCS Fit to INS Spectral Energy Distributions. T_{rad} is the initial blackbody temperature, T_e is temperature of the electron system, seen at infinity. N_e is the electron number density, “norm” is the solid angle of the source seen by the observer. Equivalent hydrogen column density n_H is the result of wabs model.

	kT_{rad} eV	kT_e eV	N_e 10^{12} cm^{-3}	norm	n_H 10^{20} cm^{-2}
J1856	61	26	1.8	$\pi(10 \text{ km}/161\text{pc})^2$	1.6
J0720	80	35.4	1.8	$\pi(10 \text{ km}/330\text{pc})^2$	2.8

the electron system, the electron number density (assuming homogenous), and a normalization constant. We want to point out that our model has the same number of free parameters as the double blackbody fit (two temperatures and two normalization constants). The RCS model parameters are given in table 2.

During the fitting process, the magnetic field and stellar radius are chosen to be typical values 10^{13} G and 10 km, respectively (e.g. Haberl 2007). In the case of J1856, the initial blackbody temperature is chosen slightly lower than the high temperature component of the double blackbody fit. The temperature of the electron system is chosen as the low temperature component of the double blackbody fit and kept fixed during the fitting process. The electron number density are assumed to be homogenous. The corresponding optical depth is about 1000. The normalization constant is the solid angle of the source seen by the observer. The photoelectric absorption cross section is from Morrison & McCammon (1983) (the wabs model). The hydrogen column density is consistent with previous studies (Burwitz et al. 2003; Ho et al. 2007).

The case of J0720 is similar. This may in part reflect the similarities between these two INSs. The optical/UV excess of INSs in our model is due to magnetospheric processes. This means that, in our model, the central star can be a normal neutron star, although other possibilities, e.g. a quark star, can’t be ruled out (Xu 2002, 2003; for a review, see Xu 2009).

In our model about the INSs, the blackbody spectrum is from the whole stellar surface. When passing through the CFLRs of the pulsar magnetosphere, the photons are down scattered by the RCS process. It will bring a decrease of high energy photons. This can account for the observed optical/UV excess. At the same time, since the X-ray emission is from the whole stellar surface, it can also explain the low pulsation amplitude naturally.

6 DISCUSSIONS

We consider the RCS process in this paper. Previous work of Ruderman (2003) is mainly qualitative consideration. While our paper is a quantitative one and detailed comparison with observational data is also presented. Lyutikov & Gavriil (2006) consider the RCS process by solving the radiation transfer equation directly. We want to point the differences between our paper and their’s.

1. An improved approximation is used. The photon system is modeled three dimensionally in our paper.

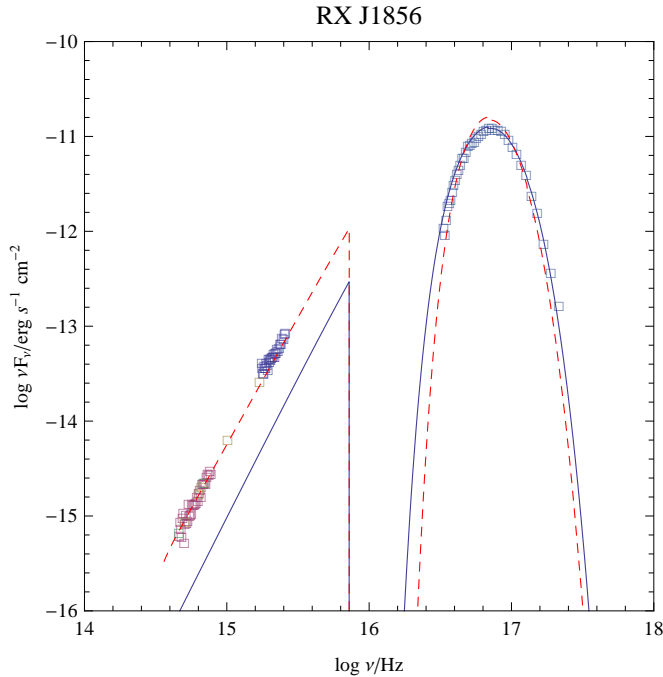


Fig. 4 Spectral energy distributions of J1856. The squares are observational points (only central values are included). The solid line is single blackbody fit to the X-ray data, the parameters are given in table 1. (It is not the initial blackbody spectrum in our model, the parameters are listed in table 2.) The dashed line is the RCS modified blackbody spectrum, the model parameters are given in table 2. The specified frequency range and model parameters are the same as that in figure 3. All observational data are from van kerkwijk & Kaplan (2007).

2. A different method is employed. While Lyutikov & Gavriil solved the radiation transfer equation directly, we employed the Kompaneets equation method. They are independent methods. The Kompaneets equation method is much simpler both analytically (compared to solving radiation transfer equation directly, this is why we can employ better approximations) and numerically (compared to doing Monte Carlo simulations).
3. Different applications are considered. Previous researchers on RCS mainly focus on its application to magnetars. We point out that it may also play an important role in the radio quiet INS case. Therefore, a magnetospheric model is presented for the optical/UV excess of INSs.
4. Our calculations show that there exist not only up scattering but also down scattering of RCS process.

Further Monte Carlo simulations may tell us more about the down scattering of RCS if there exists real down scattering of RCS. The approximation of a 1D treatment (Lyutikov & Gavriil 2006) may result in a negative point of down scattering of RCS. Our deduction is in the 3D case (for the photon system). The key difference is the phase space volume (in 1D case $\propto p$, in 3D case $\propto p^3$). While in eq. (16), we note a factor $(1 + n)$ appears. This is a pure second quantization effect. The photons are aligned to condensate in the low energy state, and this quantum effect can only play an important role in 3D case. Note that there is also no Bose-Einstein condensation in the low dimension case (see Pathria 2003).

Through this paper we talk about the RCS process in pulsar magnetospheres. We think it may be a common process. In different cases, it has different manifestations. In the case of magnetars, we have observed a stiffened blackbody spectrum. In the case of INSs, we have observed an optical/UV

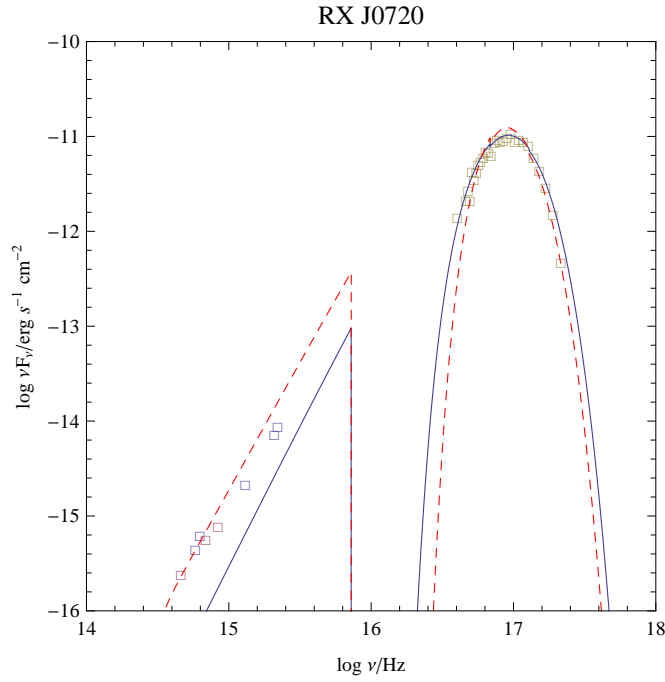


Fig. 5 Spectral energy distributions of J0720. The optical/UV data of J0720 is more likely to be nonthermal. The specified frequency range is the same as that in figure 3. The model parameters are $(x_1, x_2) = (0.042, 56)$, $(r_2, r_1) = (3.9, 42) \times 10^6$ cm. (The space range is the same as that in figure 3, since it is only determined by the specified frequency range, see eq.(9)). All observational data are from van kerkwijk & Kaplan (2007).

excess. These different manifestations can be treated universally using the Kompaneets equation for RCS presented in this paper.

Concerning the magnetospheric properties, now people are thinking about that the CFLRs of pulsar magnetospheres are not dead but filled with dense plasma (Ruderman 2003; Luo & Melrose 2007; Lyutikov 2008). The plasma can be $10^4 - 10^5$ times denser than the local Goldreich-Julian density. The origin of this over dense plasma is the presence of twisted magnetic field lines (in the case of magnetars) or magnetic mirroring (in the case of RRATs). When discussing the magnetospheric properties we have to be careful. As stated in section two, the scattering radius and the optical depth (or cross section) is frequency-dependent. The local Goldreich-Julian density is proportional to the magnetic field. At the scattering sphere, from eq.(1), it is proportional to the photon frequency. Given that the electron density is a constant, the ratio of N_e/n_{GJ} varies with frequency as $\propto 1/\nu$. In the case of magnetars (photon energy ranges between 1 keV – 10 keV), the electron density is $10^3 - 10^4$ times the local Goldreich-Julian density. While in the case of INSSs, we have a broader frequency range 1 eV – 1 keV and a much higher RCS optical depth, about 1000. The corresponding electron density is $10^3 - 10^6$ times the local Goldreich-Julian density. Therefore, a plasma with number density $10^4 - 10^5$ times the local Goldreich-Julian density is presented in the CFLRs of magnetars/INSSs according to our model. We have computed the mass of this dense plasma. Assuming an electron-ion plasma, the total mass is 10^{11} g and 10^{12} g in the magnetar case and INS case, respectively. This is consistent with studies in the double pulsar binary PSR J0737-3039, Crab giant pulses, and magnetar spectrum modeling (Lyutikov 2008; Rea et al. 2008).

The presence of dense plasmas in CFLRs of INSSs needs further explanations. Unlike the case of magnetars, the INSSs are believed to be dead NSs (Kaspi et al. 2006; Trümper 2005). For slow rotators

like INSs, the magnetic mirroring mechanism comes to work (Luo & Melrose 2007). Therefore, we think that the dense plasma in the case of INSs could be due to magnetic mirroring mechanism. The source of this dense plasma may be the result of accretion from circumpulsar material, e.g. ISM, fallback disk etc. Unlike the case of RRATs, in the case of INSs the radiation belts are not very far away from the neutron stars (about 40 stellar radii at the outer edge). We may call it the “inner radiation belt” of a pulsar if we call the radiation belt near the light cylinder proposed by Luo & Melrose (2007) the “outer radiation belt” of a pulsar. Nevertheless, the particle processes are similar. The pulsar accretes material from the environment which will be accelerated in the “dormant outer gap” (Luo & Melrose). High energy curvature photons will collide with surface X-ray photons generating pairs in INS CFLRs. The pair plasma will be confined by the magnetic mirroring mechanism. This is the pulsar “inner radiation belt” (or “electron blanket”, e.g. Ruderman 2003). Semi-quantitative estimates are given in Luo & Melrose (2007), Ruderman (2003). It can be as high as $10^4 - 10^5$ times the Goldreich-Julian density. The plasma is cold since it has undergone a long time of relaxation (INSs are old thermally emitting neutron stars). Meanwhile during the scattering process, the photons will push the plasma particles away from the star. The kinetic energy of particle decreases thus resulting in a low temperature. This also explains why the plasma system in INS CFLRs is distributed in a rather wide space range, see caption of figure 3. Similar process is also possible in corona of magnetars (Beloborodov & Thompson 2007).

The last but not least important question is: can a neutron star have a blackbody spectrum which can be modified when passing through its magnetosphere? It might not be impossible. The current neutron star atmosphere models leave us two questions: one is that a blackbody spectrum fits the observation better than that with spectra lines (Ho et al. 2007). The other is that we haven’t found a high energy tail in INS X-ray spectra (van Kerkwijk & Kaplan 2007). Therefore from the observational point of view, a blackbody spectrum is possible. A blackbody-like spectrum could be reproduced in a quark star model (Xu 2009).

7 CONCLUSIONS

We consider the RCS process in pulsar magnetospheres. The photon diffusion equation (Kompaneets equation) for RCS is presented. It can produce not only up scattering but also down scattering depending on the parameter space. Its possible applications to magnetar soft X-ray spectrum and INSs are point out.

The application to INSs is calculated in detail. We show that the optical/UV excess of INSs may be due to down scattering of RCS. The RCS model has the same number of parameters as the double blackbody model. Mean while, it has a clear physical meaning. The initial blackbody spectrum from the stellar surface is down scattered by the RCS process when passing through its magnetosphere. This can account for the optical/UV excess of INSs. The low pulsation amplitude of INSs is a natural consequence in our model.

The calculations for RX J1856.5-3754 and RX J0720.4-3125 are presented and compared with their observational data. The model parameters for RX J1856.5-3754 and RX J0720.4-3125 are similar. This may in part reflect the similarities between these two INSs. Finally, we point out that the quark star hypothesis (e.g. Xu 2002) can still not be ruled out.

The photon diffusion equation (Kompaneets equation) for RCS is calculated semi-analytically. The calculations for the magnetar and INS cases are all for surface thermal emission. Of course, its application is not limited to the thermal emission case.

Using the Kompaneets equation (both the resonant and non-resonant ones, or a unified one which will be presented in the future), a thorough and quantitative study of scattering process in pulsar magnetospheres could be possible. This can help us make clear the physical process in CFLRs of pulsar magnetospheres.

ACKNOWLEDGMENTS

The authors would like to thank van Kerkwijk very much for providing the observational data. H.T. would like to thank Yue You Ling, Liu Dang Bo for helpful discussions. H.T. would like to thank

Prof. Chou Chih-Kang very much for sharing his manuscript which is also on Kompaneets equation for resonant cyclotron scattering. H.T. and Q.H.P. are supported by NSFC (0201131077) and the Doctoral Program Foundation of State Education Commission of China. R.X.X. is supported by NSFC (10935001, 10973002), the National Basic Research Program of China (Grant 2009CB824800), and by LCWR (LHXZ200602). L.M.S. is supported by NSFC (10778604, 10773017).

Appendix A: PROPAGATION EFFECT

The validity of isotropic assumption employed in the main body is discussed. From eq.(21) to eq.(22), we employ the isotropic assumption. It is also implicitly assumed during the angular average in the numerical calculation section. Its validity is acceptable in regions not far away from the star. This is just the case at the inner edge r_2 of the “electron blanket”. However, at the outer edge r_1 , its validity needs further confirmation. Our approach to this problem is that we consider an isotropization process. From eq. (3), the angular dependence of the outgoing photons is $(1 + \cos^2 \theta')$, the same as that of cyclotron radiation. It is almost isotropic. Therefore, weakly dependent of the angle of incoming photons, the photons become isotropic through the RCS process. This provides the required isotropic photon field to be scattered by electrons nearby. The upper isotropization process is valid from one space location to another. Therefore, the isotropic assumption is valid through the whole space range, from r_2 to r_1 .

Noting that the number of photons are conserved during the scattering process. The r^{-2} dependence of the solid angle of the star is “transformed” to the photon occupation number $n(x, t)$. It will only modify the space integrated form of Kompaneets equation, eq.(31). However, since the output is not sensitive to where we introduce the r^{-2} dependence, the results should be similar. Detailed calculation is presented in below.

The energy density of the radiation field is

$$u_\nu = \frac{4\pi}{c} J_\nu, \quad (\text{A.1})$$

where J_ν is the mean intensity

$$J_\nu = \frac{1}{4\pi} \int I_\nu d\Omega, \quad (\text{A.2})$$

I_ν is the specific intensity. From the definition of photon occupation number, we have

$$u_\nu = n(\nu) \frac{8\pi\nu^2}{c^3} h\nu, \quad (\text{A.3})$$

where $n(\nu)$ is the photon occupation number in the Kompaneets equation. Combining eq. (A.1) and (A.3), we obtain the relation between mean intensity and occupation number

$$J_\nu = \frac{2h\nu^3}{c^2} n(\nu). \quad (\text{A.4})$$

For an isotropic radiation field (e.g. as we have assumed in the main text), this is just eq.(34). We consider the propagation effect for a uniformly bright sphere with brightness B_ν and radius R (e.g., Rybicki & Lightman 1979, section 1.3). The mean intensity at radius r is

$$J_\nu = \frac{1}{2} B_\nu (1 - \sqrt{1 - (R/r)^2}). \quad (\text{A.5})$$

The dilution factor is

$$\frac{J_\nu(r \gg R)}{J_\nu(r = R)} = \frac{1}{2} \left(\frac{R}{r} \right)^2. \quad (\text{A.6})$$

This is also the dilution factor for the occupation number $n(\nu)$.

Only considering the propagation effect, it will introduce a spatial dependence of the photon occupation number

$$\frac{\partial}{\partial r} r^2 n(\nu, r) = 0. \quad (\text{A.7})$$

For neutron star with surface temperature T_{rad} , the photon occupation at radius r is

$$n(\nu, r \gg R) = \frac{1}{4} \frac{1}{e^{h\nu/kT_{\text{rad}}} - 1} \left(\frac{R}{r} \right)^2. \quad (\text{A.8})$$

Besides the dilution factor, it means that only half of the photons will propagate towards the observer.

The photon occupation number now in eq. (30) is a function of frequency, time, and position $n = n(\nu, t, r)$. In order to include the dilution effect, we introduce another variable m

$$m(\nu, t) = r^2 n(\nu, t, r). \quad (\text{A.9})$$

From eq. (A.7), m only depends on frequency and time. Multiple r^2 on both sides of eq. (30) and performing a spatial integral from r_2 to r_1 , we obtain

$$\left(\frac{\partial m}{\partial t} \right)_{\text{RCS}} = \frac{kT_e}{m_e c^2} \frac{1}{x^2} \frac{\partial}{\partial x} \left\{ x^4 \frac{\tau_{\text{RCS}}}{r_1 - r_2} c g_\theta \left[\frac{\partial m}{\partial x} + m \left(1 + \frac{m}{r_{\text{RCS}}^2} \right) \right] \right\}. \quad (\text{A.10})$$

It is similar to eq. (31).

In order to make a comparison with the observational data, the flux of such a system must be calculate. It is related to the energy density

$$\begin{aligned} F_\nu &= u_\nu c \\ &= \frac{8\pi h\nu^3}{c^2} n(\nu, t, r) \\ &= \frac{8\pi h\nu^3}{c^2} \frac{m(\nu, t)}{D^2}. \end{aligned} \quad (\text{A.11})$$

Here D is distance of this source. The spectrum is proportional to $\nu^3 m(\nu, t)$. Similar results are obtained as in the main text, with similar input parameters.

There is a deep reason why the isotropic assumption is still valid in regions far away from the star. From eq. (9), low energy photons will be scattered in outer regions. At the same time, they have large cross section and optical depth, e.g. see eq. (10) and the caption of figure 3. Low energy photons will encounter strong scattering, although they are limited in a narrow beam. Related issue has already been pointed out in section two.

References

- Bloborodov, A. M., Thompson, C. 2007, ApJ, 657, 967
 Burwitz, V., Zavlin, V., Neuhauser R., et al. 2001, A&A, 379, L35
 Burwitz, V., Haberl, F., Neuhauser, R., et al. 2003, A&A, 399, 1109
 Cheng, K. S., Ho, C., Ruderman, M. A. 1986, ApJ, 300, 500
 Fernandez, R., Thompson, C. 2007, ApJ, 660, 615
 Goldreich, P., Julian, W. H. 1969, ApJ, 157, 869
 Haberl, F. 2007, ApSS, 308, 181
 Herold, H. 1979, Physics review D, 19, 2868
 Ho, W. C. G., Kaplan, D. L., Chang, P., et al. 2007, MNRAS, 357, 821
 Kaplan, D. L., van Kerkwijk, M. H. 2009, ApJ, 692, L62
 Kaspi, V. M., Roberts, M. S. E., Harding, A. H. 2006, Isolated neutron stars, in W. H. G. Lewin, and M. van der Klis ed., Compact stellar X-ray sources, Cambridge, Cambridge (arXiv: astro-ph/0402136)

- Liu, D. B., Chen, L., Ling, J. J., et al. 2004, *A&A*, 417, 381
- Luo, Q., Melrose, D. 2007, *MNRAS*, 378, 1481
- Lyutikov, M., Gavriil, F. P. 2006, *MNRAS*, 368, 690
- Lyutikov, M. 2008, *AIP Conf. Proc.*, 968, 77 (arXiv: 0708.1024)
- McLaughlin, M. A., Lyne, A. G., Lorimer D. R., et al. 2006, *Nature*, 439, 817
- McLaughlin, M. A., Lyne, A. G., Keane, E. F., et al. 2009, *MNRAS*, 400, 1431
- Morrison, R., McCammon, D. 1983, *ApJ*, 270, 119
- Motch, C., Zavlin, V., Haberl, F. 2003, *A&A*, 408, 323
- Nobili, L., Turolla, R., Zane, S. 2008, *MNRAS*, 386, 1527
- Padmanabhan, T. 2000, *Theoretical astrophysics*, Cambridge, Cambridge
- Pathria, R. K. 2003, *Statistical mechanics (2nd ed.)*, Elsevier, Singapore
- Rea, N., Zane, S., Turolla, R., et al. 2008, *ApJ*, 686, 1245
- Ross, R., Weaver, R., McCray, R. 1978, *ApJ*, 219, 292
- Ruderman, M. A., Sutherland, P. G. 1975, *ApJ*, 196, 51
- Ruderman, M. 2003, arXiv: astro-ph/0310777
- Rybicki, G. B., Lightman, A. P. 1979, *Radiative process in astrophysics*, John Wiley & Sons, New York
- Sunyaev, R. A., Titarchuk, L. G. 1980, *A&A*, 86, 121
- Thompson, C., Lyutikov, M., Kulkarni, S. R. 2002, *ApJ*, 574, 332
- Tong, H., Peng, Q. H. 2007, *ChJAA*, 7, 809
- Tong, H., Peng, Q. H., Bai, H. 2008, *ChJAA*, 8, 269
- Trümper, J. 2005, arXiv: astro-ph/0502457
- van Kerkwijk, M. H., Kaplan, D. L. 2007, *ApSS*, 308, 191
- Wang, F. Y. -H., Ruderman, M., Hapler, J. P., et al. 1998, *ApJ*, 498, 373
- Xu, R. X. 2002, *ApJ*, 570, L65
- Xu, R. X. 2003, *ApJ*, 596, L59
- Xu, R. X. 2009, *J.Phys. G: Nucl. Part. Phys.*, 36, 064010
- You, J. H., Chen, J. F., Deng, J. S., et al. 1997, *Physics Letters A*, 232, 367
- You, J. H. 1998, *Radiative process in astrophysics (2nd ed.)*, Scientific, Beijing (in Chinese)